Counterion Binding on Charged Spheres: Effect of pH and Ionic Strength on the Mobility of Carboxyl-Terminated Dendrimers

Q. R. Huang,[†] P. L. Dubin,*[,†] C. N. Moorefield,[‡] and G. R. Newkome[‡]

Department of Chemistry, Indiana University−Purdue University at Indianapolis, Indianapolis, Indiana 46202, and Department of Chemistry, University of South Florida, Tampa, Florida 33620

Received: May 11, 1999; In Final Form: September 21, 1999

Capillary electrophoresis was used to study the effect of pH on the mobility of carboxyl-terminated dendrimers ranging from generation two to five. Even though the net charge for G5 (−972) is much higher than that of G2 (−36), its electrophoretic mobility is lower. Titration studies reveal that the effective surface charge density of G5 is lower than the geometric surface charge density, which we attribute to counterion binding. The results suggest a critical condition for nonspecific counterion binding to spheres, analogous but not identical to the well-known Manning condition for counterion condensation on polyelectrolytes.

Introduction

The technological and theoretical aspects of colloidal systems have received considerable attention in the past decade.[1−4] The properties of aqueous colloidal systems are often dominated by electrostatic forces because most hydrophilic surfaces bear surface charges, either intrinsically or via adsorption of ions. Because of the long-range nature of electrostatic forces, the colloid surface charge densities, or surface potentials (ψ_0), play a major role in colloid behavior. The other primary determinant of aqueous colloidal behavior is the distribution of counterions, which can be treated effectively by some form of the linearized Poisson−Boltzmann (PB) equation in the case of small ψ_0.[5] However, the behavior of highly charged particles with large ψ_0 is complicated by specific and nonspecific "counterion binding" and hydration effects.

Verification of theories put forward in this field would benefit from studies with "ideal" colloidal particles. For this purpose, latexes are often used,[6−9] but latex charges usually arise from ionic surfactant adsorbed during preparation, with the other regions of the latex being hydrophobic. The exact nature and distribution of the charge sites are problematic, and the existence of "buried charges" is difficult to preclude.

Dendrimers are densely branched molecules of well-defined (spherical or nearly-spherical) geometry.[10,11] Carboxyl-terminated dendrimers thus resemble spheres whose uniform surface charge densities can be modulated continuously by pH, and their radii can be varied synthetically from 1 to 5 nm.[12,13] Recently, we have characterized small dendrimers by potentiometric titration and dynamic light scattering and found perfect adherence to the PB equation under conditions of low charge.[14] However, for carboxyl-terminated dendrimers of higher generation (generation number ≥ 2), the electrostatic coupling between oppositely charged species induces a strong accumulation of counterions (or counterion binding) in the vicinity of the macroion surface. As a consequence, the effective surface charge density is much weaker than the apparent geometric (or "structural") surface charge density.[14]

Although the theory by Manning[15] about counterion condensation around a rodlike polyelectrolyte is well-recognized, the idea of counterion condensation around a spherical charged particle is still controversial. According to Zimm and Le Bret,[16] charged spheres have no condensed counterions, whereas all counterions are condensed for charged planes. The notion of an effective charge Q_{eff} (as opposite to the geometric charge Q_{geom}) is widely used in the literature and is a powerful concept to illustrate the strong accumulation of counterions in the vicinity of the spherical particles. The electrokinetic properties, such as the potential at the surface of shear ("ζ potential"), are closely related to Q_{eff} instead of Q_{geom}. However, the ζ potential is not easily related to the surface potential. An understanding of the ζ potential is of importance in determining, for example, the stability, rheological properties, and coating behavior of colloidal suspensions. The ζ potential cannot be measured directly, but it can be related to the electrophoretic mobility, defined as the velocity the particle attains per unit electric field. Such relationships, however, are model-dependent. Since the pioneering work of Smoluchowski,[17] there have been many theoretical descriptions of electrophoresis of spherical particles.[18−23] However, experimental data for the case of highly charged spherical particles are still very scarce, especially data that demonstrate the relationship between the electrophoretic mobility and the surface charge density of the macroparticles. The sphericity, monodispersity, and uniform surface charge density of carboxyl-terminated dendrimers make them particularly suitable for such fundamental electrokinetic studies.

The application of capillary electrophoresis (CE) to the measurement of mobility is relatively new but shows considerable promise.[24,25] Encouraged by the high efficiency and rapid analysis offered by free-zone CE, we set out to investigate the effect of counterions on the mobility of the carboxyl-terminated dendrimers. The present paper focuses on the dependence of the electrophoretic mobility on pH and ionic strength for dendrimers with radii in the range of 15−40 Å.

Experimental Section

Materials. Carboxylic acid-terminated cascade polymers (Z-Cascade:methane[4]:(3-oxo-6-oxa-2-azaheptylidyne):(propanoic acids)) of generations 2−5 (hereafter referred to as dendrimers) were synthesized by procedures described elsewhere.[12] G4 and G5 were further purified by dialysis (Spectra/Por dialysis

[†] Indiana University−Purdue University at Indianapolis.
[‡] University of South Florida.

10.1021/jp991545m CCC: $19.00
Published on Web 01/19/2000

TABLE 1: Characteristics of Carboxyl-Terminated Cascade Polymers

generation	no. of terminal COOH	MW	hydrodynamic radius (nm)[a]	surface charge density (C/m^2)[b]
2	36	4 092	1.7	0.16
3	108	12 345	2.4	0.24
4	324	37 102	3.3	0.38
5	972	111 373	3.7	0.94

[a] From Young et al.,[13] at neutral pH. [b] Geometric surface charge density for fully ionized dendrimers.

membrane with molecular weight cutoff equal to 1000), followed by freeze-drying. Table 1 shows the characteristics of these materials.

Standard NaOH (0.1 N) and HCl (0.1 N) solutions and analytical grade NaCl were purchased from Fisher Scientific (Pittsburgh, PA). Tetramethylammonium chloride (TMACl, purity≥ 97%) was from Aldrich Chem. (Milwaukee, WI). Analytical grade sodium phosphate dibasic was from J. T. Baker Chemical Co. (Phillipsburg, NJ) and sodium phosphate monobasic was from Mallinckrodt Inc. (Paris, KY). Milli-Q water was used throughout this work.

Capillary Electrophoresis. Experiments were carried out at ionic strengths ranging from 0.005 to 0.1 M (NaH_2PO_4/Na_2HPO_4). For each buffer solution, the global buffer concentration was calculated taking into account the effect of pH. CE was carried out on a Beckman P/ACE 5500 instrument using a 50 μm inner diameter uncoated capillary, 27 cm in total length, and with a 19.25 cm effective length (from the injection end to the detection window). Because the dendrimers were found to adsorb on the capillary at low pH, all experiments were done at pH >5.5. The voltage range applied across the capillary was 10−20 kV, depending on the ionic strength of the solutions. The temperature was maintained at 25.0 ± 0.1 °C with fluorocarbon coolant. Sample injection time was 5 s with UV detection at 214 nm. Duplicate runs of each sample showed that the electrophoretic mobility, μ_E, calculated by subtracting the electroosmotic flow (EOF) of the run buffer from the sample's apparent electrophoretic mobility, was reproducible to within 2%. The electrophoretic mobility μ_E was calculated from

$$\mu_E = \frac{\nu_0 - \nu_1}{E} = \frac{lL}{V}\left(\frac{1}{t_m} - \frac{1}{t_s}\right) \quad (1)$$

where ν_0 and ν_1 are the electroosmotic velocity and the solute velocity, respectively. E is the applied electric field strength, l is the effective length of the capillary, L is the total length of the capillary (both in cm), V is the applied voltage, and t_m and t_s are retention times of the reference marker (mesityl oxide) and the sample, respectively.

Potentiometric Titration. pH titrations were conducted with a Beckman Φ34 pH meter equipped with a combination electrode (Beckman) under nitrogen atmosphere at 25 ± 1 °C. All titrations were accompanied by a dendrimer-free blank.

Calculations. The relationship between the apparent dissociation constant K_a and the degree of ionization α of the carboxylic groups of a polyacid is

$$pK_a = pH + \log\left(\frac{1-\alpha}{\alpha}\right) \quad (2)$$

where α is defined as

$$\alpha = \frac{[-COO^-]}{[COOH] + [-COOH^-]} \quad (3)$$

The pK_a of a polyacid solution can be described as[26,27]

$$pK_a - pK_0 = 0.434\frac{dG}{d\alpha}/RT \quad (4)$$

where pK_0, the intrinsic dissociation constant, is obtained by extrapolating pK_a to α = 0 and (dG/dα) is the electrostatic Gibbs free energy per unit degree of dissociation, which can be related to the surface potential by

$$\frac{dG}{d\alpha} = -eN_A\psi_0(\alpha) \quad (5)$$

where e is the elemental electric charge and N_A is Avogaro's number. Combining eqs 4 and 5, we obtain

$$pK_a - pK_0 = 0.434e\psi_0(\alpha)/kT \quad (6)$$

Thus, the surface potential $\psi_0(\alpha)$ at the site where H^+ originates can be experimentally obtained via eq 6.

For spherical colloidal particles, the complete Poisson−Boltzmann equation, in the case of 1:1 electrolyte ($Z_+ = Z_- = 1$), can be described as

$$\frac{1}{r^2}\frac{d}{d}\left(r^2\frac{d\psi}{dr}\right) = \frac{2n^0e}{\epsilon_0\epsilon_r}\sinh\left(\frac{e\psi}{kT}\right) = \frac{2000IN_A}{\epsilon_0\epsilon_r}\sinh\left(\frac{e\psi}{kT}\right) \quad (7)$$

with boundary condition

$$\frac{d\psi}{dr}|_{r=a} = -\frac{\sigma}{\epsilon_0\epsilon_r} \quad (8)$$

and

$$\psi(r \rightarrow \infty) = 0 \quad (9)$$

where I is the ionic strength, N_A is Avogadro's number, e is the elementary charge in coulombs, a is the radius, ϵ_r is the dielectric constant (here set at 78.5), ϵ_0 is the permittivity of a vacuum, k is the Boltzmann constant, and σ is the surface charge density (C/m^2). The PB equation for the potential distribution around a spherical colloidal particle in a electrolyte solution has not been analytically solved except in the limit of Debye−Huckel approximation where small potential is allowed. Loeb et al.[28] tabulated numerical solutions to the spherical PB equation. On the basis of their numerical tables, they also discovered an empirical formula for the relationship between surface charge density and surface potential of a spherical particle in 1:1 electrolytes: at T = 298K, in which the surface charge density can be described as $\sigma = 5.8718(I)^{1/2}I_0 \times 10^{-2}$ C/m^2. I_0 is the charge distribution function, which is a function of both reduced distance $q_0 = \kappa a$ and reduced potential $y_0 = e\psi_0/kT$, and can be found from Table 4.1 in Loeb et al.[28] κ is the Debye−Huckel parameter, which is equal to $3.288(I)^{1/2}$ (nm^{-1}) at T = 298 K. The surface charge density deduced from the P−B equation, using the experimental surface potential ψ_0, is called the "effective surface charge density", σ_{eff}.

Results and Discussion

Figure 1 shows typical electropherograms for G2−G5 in pH = 8.66 and I = 0.06 M (κ = 0.80 nm^{-1}) Na_2HPO_4/NaH_2PO_4 buffer. All of the solutes migrate toward the negative electrode; i.e., the electroosmotic velocity is always higher than the

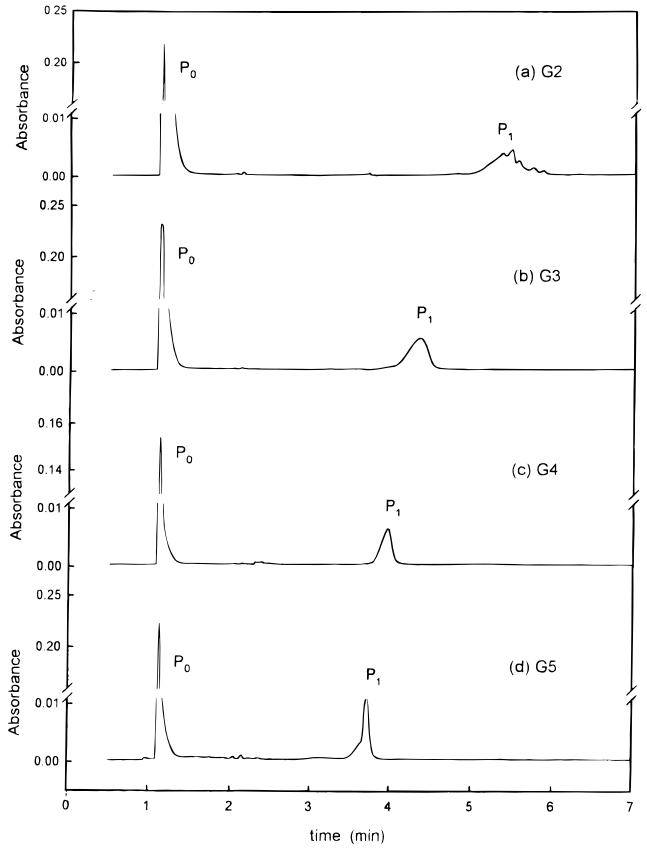

Figure 1. Electropherogram of dendrimers of different generation number in pH = 8.66 and I = 0.06 M sodium phosphate buffer: (a) G2, (b) G3, (c) G4, and (d) G5.

solute electrophoretic velocity under the conditions shown in Figure 1. There are two peaks in each curve: neutral marker peak (P_0) and dendrimer peak (P_1). With the increase of dendrimer generation number, P_1 shifts to shorter time. Because the dendrimer is negatively charged, decrease in the elution time indicates a decrease in mobility.

Figure 2 shows the pH dependence of both neutral marker electroosmotic velocity (ν_0) (often called "EOF") and the solute velocity (ν_1). One notes that electroosmotic velocity increases monotonically with increase of pH, but the solute velocity shows a local minimum at pH around 7. The observed velocity of the solute is primarily affected by two factors: the electroosmotic flow and the true electrophoretic mobility. Because the latter is more interesting, we correct ν_1 for the contribution from the electroosmotic effect.

The degree of ionization α of the carboxylic groups defined in eq 3, which is directly related to the surface charge density of the carboxyl-terminated dendrimer, can be modulated continuously by pH and can be obtained from potentiometric titration. Because the dendrimers adsorbed to the capillary at low pH, we carried out the CE measurements only at pH > 5.5 ($\alpha > 0.4$). Figure 3 shows the α dependence of the true electrophoretic mobility μ for G2 and G5 in I = 0.05 M Na_2HPO_4/NaH_2PO_4 buffer solution ($\kappa = 0.73$ nm^{-1}). An interesting feature is the local maximum for both G5 and G2 at $\alpha = 0.81$ and 0.92, respectively, prior to which the mobility is nearly linear with α. Thus, for either G5 or G2, it is possible for two macroparticles of the same size but with different charges (e.g., G5 at $\alpha = 0.7$ and $\alpha = 1.0$) to have the same electrophoretic mobility. But the most remarkable observation in Figure 3 is that the mobility for G2 is always larger than that of G5 despite the fact that the latter has a net charge 27 times larger (972 vs

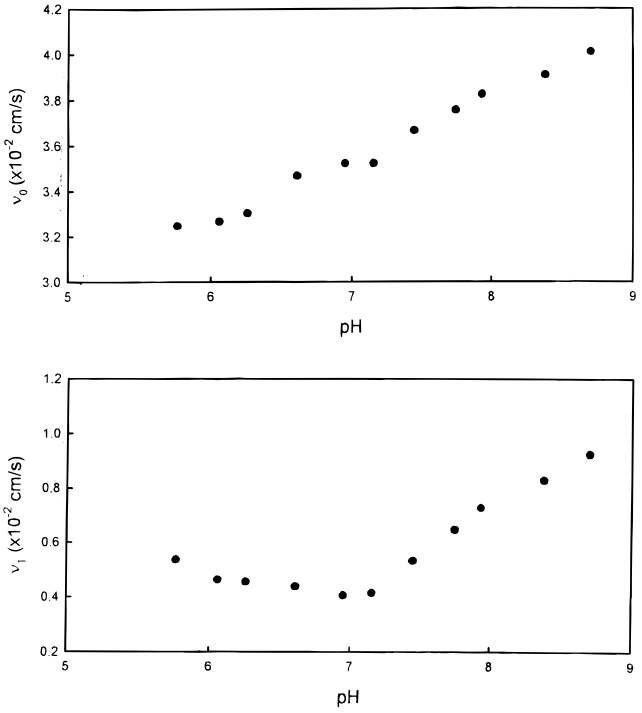

Figure 2. pH dependence of the electroosmotic velocity (top) and the apparent velocity of G2 (bottom) at I = 0.05 M sodium phosphate buffer.

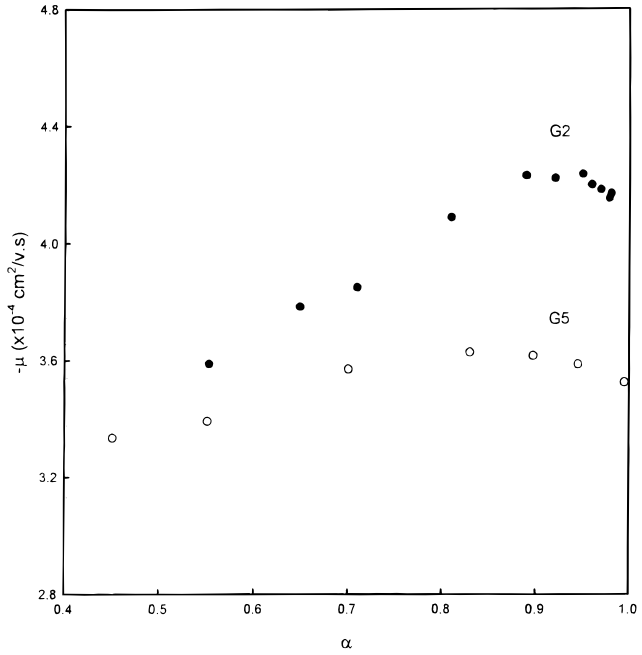

Figure 3. Dependence of mobility on α for G2 (solid circles) and G5 (open circles) in pH = 0.05 M sodium phosphate buffer.

36). This observation is also confirmed in Figure 4, which shows the ionic strength dependence (κ ranging from 0.23 to 1.04 nm^{-1}) of the mobility for G2−G5 at pH = 8.66 ($\alpha = 1$). The mobility always decreases with increase of ionic strength, but for any fixed ionic strength, the mobility decreases with increase of dendrimer generation number.

To summarize, capillary electrophoresis shows two interesting phenomena: (1) a local maximum for the mobility versus α, and (2) a decrease in mobility with increase of dendrimer generation number at any ionic strength. Turning first to the maximum in μ at $\alpha \cong 0.8$, we note that nonlinear relationships

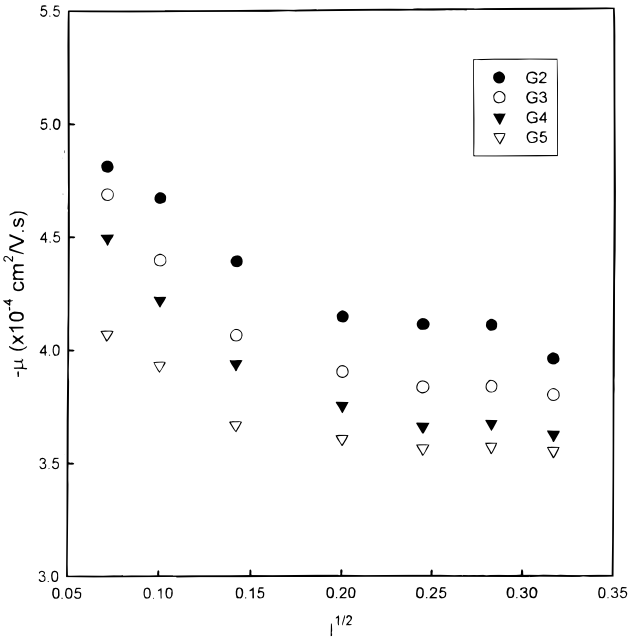

Figure 4. Ionic strength dependence of mobility for G2 (solid circles), G3 (open circles), G4 (solid inverted triangles), and G5 (open inverted triangles) at pH = 8.66.

between mobility and surface charge density have also been predicted by two theories: that of Wiersema[19] and O'Brien and White[20] (WOW), and the restricted primitive model (RPM) by Lozada-Cassou et al.[21−23] WOW consider the deformation of the ionic cloud around the moving macroparticle (relaxation effect) and assume that the macroparticle is a hard sphere with a uniform surface charge density and that the surrounding counterions are point ions. According to WOW,[20] there are three forces that will affect the mobility: (1) an electric force propelling the macroparticles that depends on the number of charges; (2) a force due to hydrodynamic drag that depends on radius, viscosity, etc.; and (3) a relaxation force originating from the induced polarization within the diffuse layer of ions surrounding the maroparticles. WOW does predict maxima in the dependence of mobility on surface charge, but only for $\kappa a > 3$, whereas we find maxima for G2 when κa is as low as 1.25. RPM models the surrounding counterions as hard spheres of finite size and consequently predicts that the mobility at a fixed ζ potential (ζ) depends not only on κa but also on the size of the macroparticles.[29] When the radius of the macroparticles is on the same order as that of the small ions, the $\mu_E(\zeta)$ relationship dramatically deviates from the WOW result, and a local mobility maximum occurs at a lower ζ.[29] RPM thus may qualitatively predict our observed maximum in μ_E versus α. Comparisons between RPM theory and experiment are however tangential to the main point of this work, the larger mobility for the smaller dendrimer.

Although WOW does not seem to predict the correct presence of maxima in $\mu_E(\zeta)$ at small κa, we may still attempt to use it to predict the relative mobilities of G5 and G2. To do so, we consider first their expected ζ potentials. For G2 and G5, respectively, the formal surface charge densities at full ionization ($\alpha = 1$), $\sigma_{geom} = eN_t\alpha/4\pi a^2$, where N_t is the number of total ionizable group on the dendrimers, are 0.16 and 0.94 C/m^2. The ζ potential can be approximated by

$$\zeta = \frac{\sigma_{geom} a}{\epsilon_r \epsilon_0 (1 + \kappa a)} \qquad (10)$$

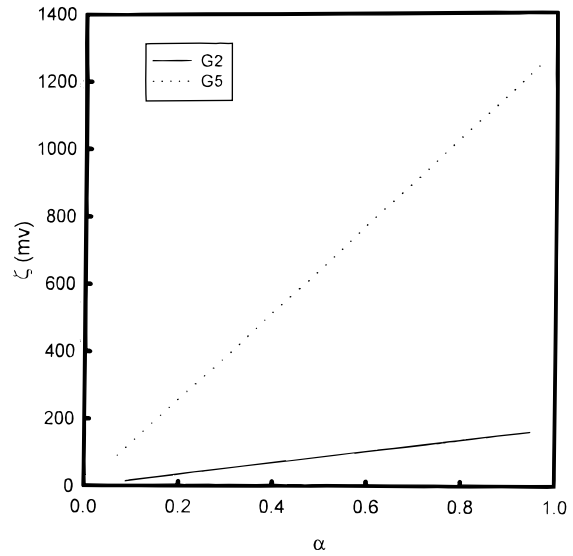

Figure 5. The plot of estimated ζ potential from the net charge of the dendrimers using $\zeta = N_t e\alpha/4\pi\epsilon_r\epsilon_0(1 + \kappa a)a$ vs α for G2 and G5.

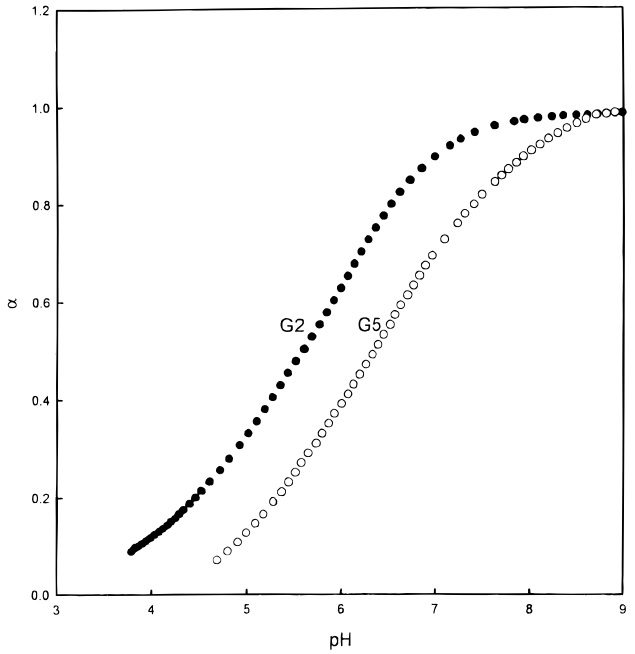

Figure 6. pH titration curves for G2 (solid circles) and G5 (open circles) in $I = 0.05$ M NaCl.

Although this equation is strictly correct only for low ζ,[30] the qualitative result, shown in Figure 5, makes it clear that ζ should be larger for G5 than G2 at high pH, in conflict with the experimental result that the mobility of G2 is 20% larger than that for G5. A second inconsistency is that WOW predicts that the mobility should be constant for $\zeta > 450$ mV, which according to Figure 5 occurs at $\alpha > 0.4$; however, from Figure 3, μ_E apparently continues to increase up to $\alpha = 0.9$.

The unreasonably high ζ estimated from eq 10 leads us to consider the possibility of effective charge densities different from σ_{geom}. Fortunately, effective surface charge densities can be calculated from surface potentials that are readily obtained by potentiometric titration. Typical titration curves for G2 and G5 at $I = 0.05$ M NaCl are shown in Figure 6. Although both curves converge with full ionization, one immediately notes the higher degree of ionization α for G2 versus G5 at any pH, which indicates that G2 is a stronger acid than G5. This difference

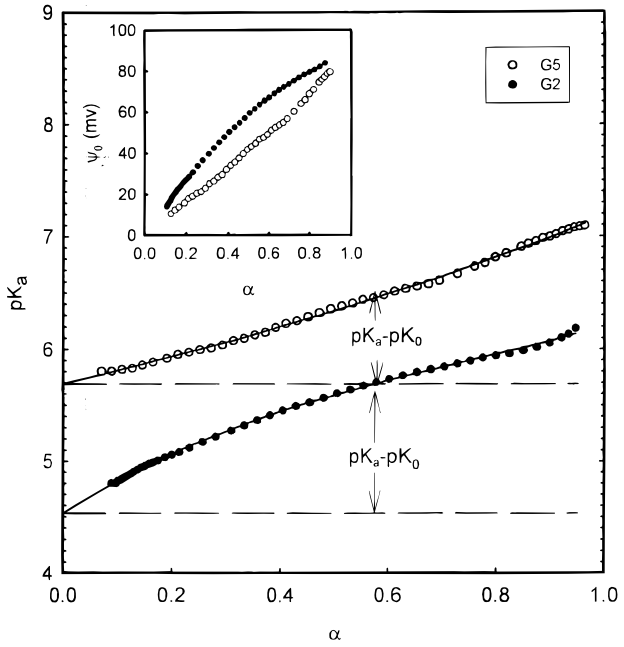

Figure 7. Dependence of pK_a on α in $I = 0.05$ M NaCl. The inset is the plot of surface potential (ψ_0) vs α.

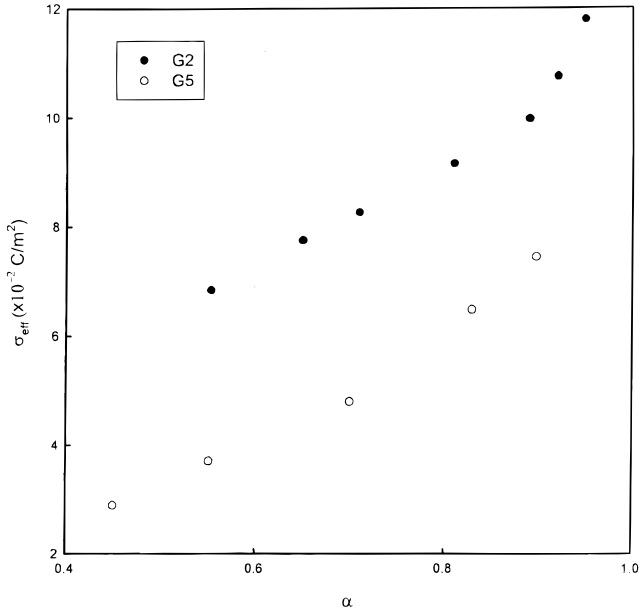

Figure 8. Dependence of effective surface charge density on α for G2 (solid circles) and G5 (open circles) in pH = 0.05 M NaCl.

can be examined more quantitatively by the plots of $pK_a = pK_0 + \log(\alpha/1-\alpha) = pK_0 + 0.434e\psi_0(\alpha)/kT$ shown in Figure 7. The plot of ψ_0 versus α shown in the inset for $0.1 < \alpha < 0.9$ (the experimental error in pK_a is large beyond these limits) reveals that ψ_0 is only 10% of the estimated ζ potential. Interestingly, pK_a − pK_0 ∼ ψ_0 is larger by some 20% for G2 than that for G5, which is identical to the differences in μ_E noted above.

It is possible to convert the surface potential ψ_0 to an effective surface charge density σ_{eff} by using eqs 7−9. The results are presented in Figure 8 as the α dependence of σ_{eff}. In distinction from the structural surface charge density σ_{geom}, σ_{eff} is the surface charge density deduced from the P−B equation using the experimental surface potential $\psi_0(\alpha)$. At any α value, σ_{eff} is higher for G2, even though σ_{geom} is 6 times larger for G5. The low effective surface charge density of G5 must be due to

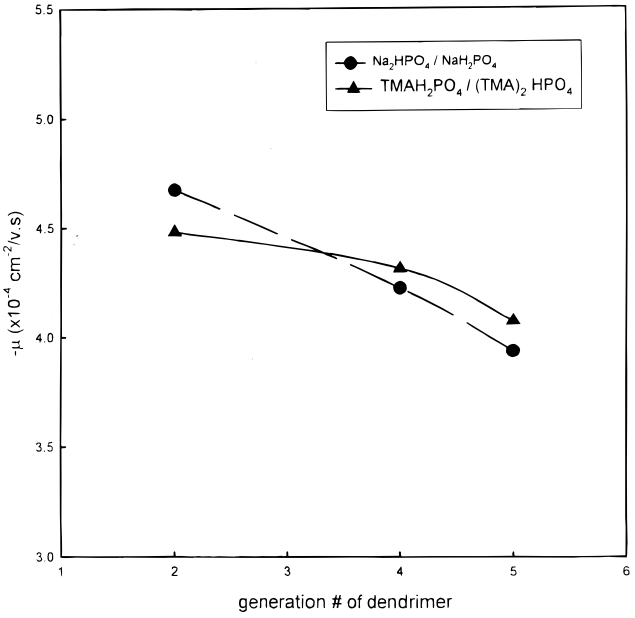

Figure 9. Dependence of mobility on the dendrimer generation number in pH = 8.66 and $I = 0.01$ M sodium phosphate (solid circles) and tetramethylammonium phosphate (solid triangles) buffer solutions

binding of counterions at its surface, which may be either "specific" or "nonspecific". Specific ion-binding effects for polycarboxylates are well-known,[31] and a variety of dilatometric and potentiometric studies have confirmed that the order of binding for polycarboxylic acids is $Li^+ > Na^+ \sim K^+ \gg TMA^+$.[32] To distinguish between these two types of binding, we carried out mobility measurements of G2, G4, and G5 in pH = 8.66 and $I = 0.01$ M sodium phosphate and tetramethylammonium phosphate buffer solutions, as shown in Figure 9. The results show that the mobility decreases with increase of the dendrimer generation number in the presence of either Na^+ or TMA^+, which indicates that nonspecific ion-binding is the main reason for the lower effective surface density of G5.

Counterions located at short enough distances from a highly charged colloidal surface feel a large electrostatic attraction.[33] The surface potential ψ_0 of a charged sphere of radius a with Q charges is $\psi_0 = Qe/4\pi\epsilon_0\epsilon_r a$, and the electrostatic energy of the counterion at this distance is $U_{counterion} = e\psi_0 = Qe^2/4\pi\epsilon_0\epsilon_r a$. A counterion may be considered to be strongly bound to any surface if the attraction energy is much higher than the thermal energy kT, i.e.

$$U_{counterion} = \frac{Qe^2}{4\pi\epsilon_0\epsilon_r a} \gg kT \tag{11}$$

or

$$\frac{l_b Q}{a} \gg 1 \tag{12}$$

where $l_b = e^2/4\pi\epsilon_0\epsilon_r kT$ is the Bjerrum length. This condensation criterion for colloids is analogous to Manning's criterion for linear polyelectrolytes.[15] Although the terms "binding" and "condensation" are sometimes used interchangeably, the meaning of condensation is the occurrence of binding only when the macroion geometric (or structural) charge density exceeds a critical threshold value. Equation 12 describes the condition at which the binding of counterions may resemble their localization near a charged plane. For spheres, localization will occur as long as[33,34]

$$\frac{a^2}{l_b Q_{geom}} \ll \frac{1}{\kappa} \quad \text{or} \quad \frac{l_b Q_{geom}}{a} \gg \kappa a \tag{13}$$

where $1/\kappa$ is the Debye screening length. Figure 10 shows the plot of $l_b Q_{geom}/a$ versus α for four different dendrimers. One notes the dramatic increase in $l_b Q_{geom}/a$ with increase of generation number, which corresponds according to eq 11 to an increase in bound counterions. For G2, at $I = 0.05$ M and $\alpha > 0.4$, $\kappa a = 1.25$, and $l_b Q_{geom}/a > 6$, whereas for G5, $\kappa a = 2.72$ and $l_b Q_{geom}/a > 70$. Thus, the condition of eq 13 is clearly met for G5. The large mobility for G2 versus G5 can be understood if we compare the dependence of mobility on effective surface charge density for the two dendrimers, as in Figure 11. The primary effect is the depression of the effective surface charge density of G5, which we ascribe to counterion binding. Indeed, the mobilities of G2 and G5 are similar when their effective surface charge densities are similar.

The potentiometric curves of Figure 7 indicate that pK_0 is larger for G5 than for G2. The quasilinear dependence of pK_a on α is very much as expected for a uniformly charged sphere,[35] which facilitates extrapolation to $\alpha = 0$. Therefore, the values of pK_0 can be reported with reasonable confidence as 5.70 ± 0.05 and 4.60 ± 0.10, i.e., a large increase in pK_0 with dendrimer size. Indeed, at ionic strength 0.05 M, pK_0 increases with increasing dendrimer generation number, as shown in Figure 12. This unexpected result may be related to the formation of intermolecular hydrogen bonds (between undissociated carboxyl groups), which could weaken the acidity at $\alpha = 0$. Such hydrogen bonding would be favored by the increase in COOH surface density with dendrimer size, because every increase of generation number increases the number of carboxylic acid groups by a factor of 3, whereas surface area increases by a factor of less than 2.

A final observation from Figure 11 is the flattening of the effect of σ_{eff} on μ at larger σ_{eff}, which may be related to counterion condensation within the shear plane. Because the effective surface charge ($Q_{eff} = 4\pi a^2 \sigma_{eff}$) is the parameter best correlated with the accumulation of counterions around the colloidal particles, we plot the mobility versus $Q_{eff} l_b/a$ in the inset of Figure 11. The physical meaning of this renormalization is similar to that of eqs 10 and 11: it is the ratio of the energy of electrostatic attraction between counterions and the dendrimer surface to the thermal energy. This parameter controls counterion condensation. The inset of Figure 11 shows that, for both G2 and G5, a break point in mobility occurs when $Q_{eff} l_b/a > 9$. By numerical solution of the P−B equation, Belloni[33] also observed an inflection in the concentration profile of counterions around charged spheres (in 1:1 electrolyte) when $Q_{eff} l_b/a > 4$, which he identified as the condition for counterion condensation. This result is quite similar to our findings. However, Belloni's definition of condensed counterions includes counterions within a significant distance from the particle surface. Although the ions this far from the surface may not contribute to a depression in our measured ψ_0, the Belloni model serves to indicate that the ψ_0- and ζ-determining ions need not be exactly at the particle surface. In this respect, the binding proposed here is different from the Manning model and need not lead to constant mobility at high charge density as is observed theoretically[15] and experimentally[36] for linear polyelectrolytes. A similar break point in the mobility can also be seen for flexible linear polyelectrolytes[36] when the linear charge density ξ exceeds the Manning critical value corresponding to the onset of counterion condensation. However, the fundamental resemblance of the two phenomena remains to be elucidated.

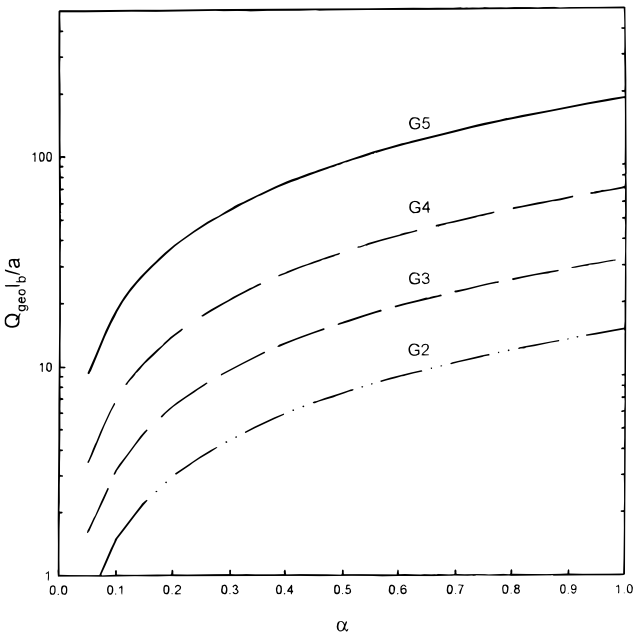

Figure 10. Dependence of $Q_{geom} l_b/a$ on α for G2−G5.

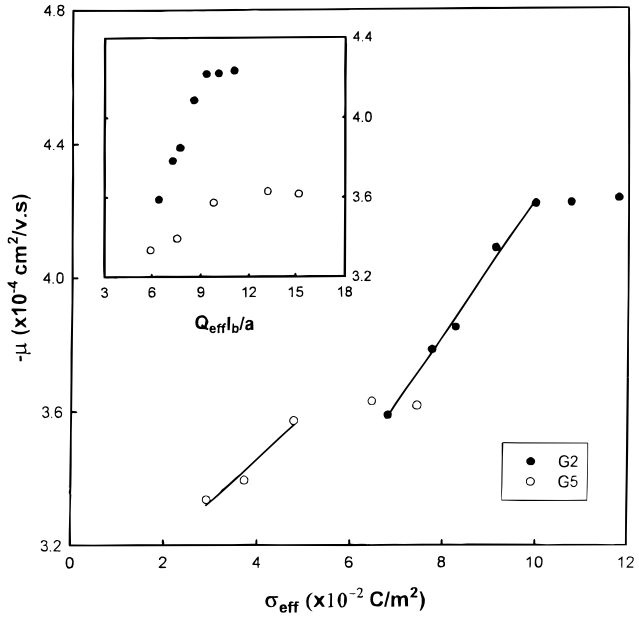

Figure 11. Dependence of mobility on effective surface charge density for G2 (solid circles) and G5 (open circles) in pH = 0.05 M sodium phosphate buffer. Data at high σ are omitted due to experimental uncertainty. Inset: dependence of mobility on $Q_{eff} l_b/a$.

Conclusions

We have carried out capillary electrophoresis studies of the effect of counterions on the mobility of carboxyl-terminated dendrimers with dendrimer generation number ranging from 2 to 5, in particular examining the pH and ionic strength dependence of the electrophoretic mobility. The two most significant results are as follows: (1) a decrease in mobility with increase of dendrimer generation number at any ionic strength and (2) a local maximum for the mobility versus the degree of ionization α at $\kappa a < 3$. Potentiometric titration results show that even though the geometric charge for G5 (−972) is much higher than that for G2 (−36), the effective surface charge density for G5 is actually lower, presumably due to counterion binding. Under conditions where G2 and G5 have the same effective charge density, their mobilities are similar. The local

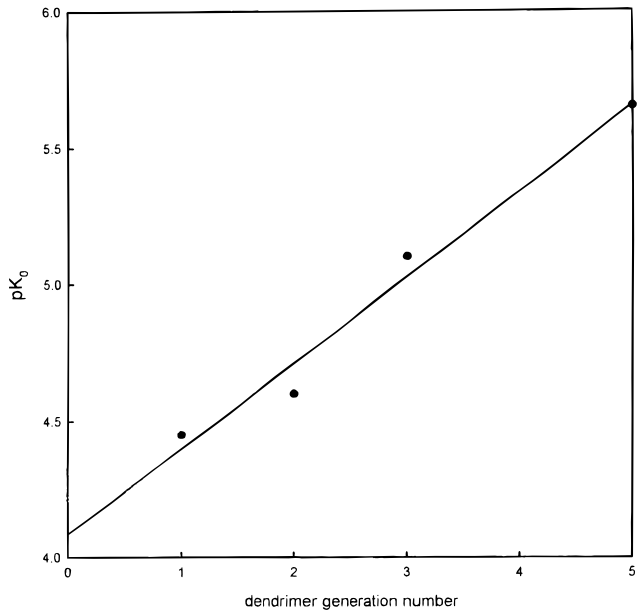

Figure 12. Dependence of pK_0 on dendrimer generation number.

maximum for the mobility versus α at $\kappa a < 3$ may be predicted by the "restricted primitive" model of Lozada-Cassou.

Acknowledgment. This work was supported by the Petroleum Research Fund (PRF32625-AC7) and the National Science Foundation (Grants DMR9311433 (P.L.D.) and DMR9622609 (G.R.N.)). We thank Professors A. Dobrynin and M. Lozada-Cassou for helpful discussions.

References and Notes

(1) *An Introduction to Polymer Colloids*; Candau, F., Ottewill, R., Eds.; Kluwer Academic: The Netherlands, 1990.
(2) Evans, D. F.; Wennerstrom, H. *The Colloidal Domain*, 2nd ed.; John Wiley & Sons: New York, 1999.
(3) Hunter, R. J. *Foundations of Colloid Science*; Oxford University Press: Oxford, 1987; Vol. 1.
(4) *The Structure, Dynamics and Equilibrium Properties of Colloidal Systems*; Bloor, D. M., Wyn-Kones, E., Eds.;; NATO ASI Series; Kluwer Academic: Boston, 1990.
(5) Debye, P. J. W.; Huckel, E. *Phys. Z.* **1923**, *24*, 185.
(6) Chow, R. S.; Takamura, K. *J. Colloid Interface Sci.* **1988**, *125*, 226.
(7) Elimelech, M.; O'Melia, C. *Colloids Surf.* **1990**, *44*, 165.
(8) Verdegan, B. M.; Anderson, M. A. *J. Colloid Interface Sci.* **1993,** *158*, 372.
(9) Folkersma, R.; van Diemen, A. J.; Stein, H. N. *Langmuir* **1998**, *13*, 5973.
(10) Newkome, G. R.; Moorefield, C. N. In *Advances in Dendritic Macromolecules*; Newkome, G. R., Ed.; JAI Press: Greenwich, CT, 1993; Chapter 1.
(11) Newkome, G. R.; Moorefield, C. N.; Vogtle, F. *Dendritic Molecules-Concepts, Syntheses, Perspectives*; VCH Publishers: Weinhein, Germany, 1996.
(12) Newkome, G. R.; Moorefield, C. N.; Baker, G. R.; Potter, R. L.; Audoly, L.; Cooper, D.; Weis, C. D.; Morris, K.; Johnson, C. S., Jr. *Macromolecules* 1993, *26*, 2394.
(13) Young, J. K.; Baker, G. R.; Newkome, G. R.; Morris, K. F.; Johnson, Jr., C. S. *Macromolecules* **1994**, *27*, 3464.
(14) Zhang, H.; Dubin, P. L.; Kaplan, J.; Moorefield, C. N.; Newkome, G. R. *J. Phys. Chem.* **1997**, *101*, 3494.
(15) Manning, G. S. *J. Chem. Phys.* **1969**, *51*, 924.
(16) Zimm, B. H.; Le Bret, M. *J. Biomolecular Struct. Dynamics* **1983**, *1*, 461.
(17) Smoluchowski, M. von, *Bull. Acad. Sci. Cracovie, Classe Sci. Math. Natur.* **1903**, *1*, 182.
(18) Henry, D. C. *Proc. R. Soc. Lond.* A. **1931**, *133*, 106.
(19) Wiersema, P. H.; Loeb, A. L.; Overbeek, J. Th. G. *J. Colloid Interface Sci.* **1966**, *22*, 78.
(20) O'Brien, R. W.; White, L. R. *J. Chem. Soc., Faraday Trans. 2* **1978**, *93*, 3761.
(21) Gonzalez-Tovar, E.; Lozada-Cassou, M. *J. Phys. Chem.* **1989**, *93*, 3761.
(22) Degreve, L.; Lozada-Cassou, M. *Mol. Phys.* **1995**, *86*, 759.
(23) Degreve, L.; Lozada-Cassou, M.; Sanchez, E. Gonzalez-Tovar, E. *J. Chem. Phys.* **1993**, *98*, 8905.
(24) Grossman, P. D.; Soane, D. S. *Anal. Chem.* **1990**, *62*, 1592.
(25) Menon, M. K.; Zydney, A. L. *Anal. Chem.* **1998**, *70*, 1581.
(26) Katchalsky, A.; Gillis, J. *Rec. Trav. Chim. Pays-Bas* **1949**, *68*, 879.
(27) Arnold, A.; Overbeek, J. Th. G. *Rec. Trav. Chim. Pays-Bas* **1950**, *69*, 192.
(28) Loeb, A. L.; Overbeek, J. Th. G.; Wiersema, P. H. *The Electrical Double Layer Around a Spherical Colloid Particle*; MIT Press: Cambridge, MA, 1961; p 40.
(29) Lozada-Cassou, M.; Gonzalez-Tovar, E.; Olivares, W. *Phys. Rev. E.*, accepted for publication.
(30) Hunter, R. J. *Zeta Potential in Colloid Science: Principles and Applications*; Academic Press: London, 1986.
(31) Gregor, H. P. In *Polyelectrolytes*; Selegny, E., Ed.; Reidel: Dordrecht, 1974; p 87D.
(32) (a) Strauss, U. P.; Leung, Y. P. *J. Am. Chem. Soc.* **1965**, *87*, 1476. (b) Begala, A. J.; Strauss, U. P. *J. Phys. Chem.* **1972**, *76*, 254. (c) Eldridge, R. J.; Treloar, F. E. *J. Phys. Chem.* **1976**, *80*, 1513. (d) Strauss, U. P.; Schlesinger, M. S. *J. Phys. Chem.* **1978**, *82*, 571.
(33) Belloni, L. *Colloids Surf. A.* **1998**, *140*, 227.
(34) Dobrynin, A., private communication.
(35) Tanford, C.; Swanson, S. A.; Shore, W. S. *J Am. Chem. Soc.* **1955**, *77*, 6414.
(36) Gao, J. Y.; Dubin, P. L.; Sato, T.; Morishima, Y. *J. Chromatogr.* **1997**, *766*, 233.